



## On the metastability of $\beta$ phase in isotactic polypropylene: experiments and numerical simulation

Paweł Sajkiewicz, \* Arkadiusz Gradys, Andrzej Ziabicki, Beata Misztal-Faraj

\*Polish Academy of Sciences, Institute of Fundamental Technological Research, Polish Academy of Sciences, Pawińskiego 5B, 02-106 Warsaw, Poland; tel: +48 22 8269815, e-mail: psajk@ippt.gov.pl

(Received: 11 December, 2009; published: 11 November, 2010)

**Abstract:** Phase transitions in isotactic polypropylene were investigated during isothermal crystallization and heating after isothermal crystallization using various experimental techniques. The results obtained by wide angle x-ray scattering (WAXS), light depolarization technique (LDT), differential scanning calorimetry (DSC) and optical microscopy show that crystallization of isotactic polypropylene can result in simultaneous formation of two crystal modifications,  $\alpha$  and  $\beta$ . There is clear experimental evidence that  $\beta$  phase tends to convert into  $\alpha$  modification during crystallization as well as during subsequent heating. Experimental results are compared with numerical simulation performed according to the model of nucleation-controlled phase transitions in multiphase systems. The results of simulation show that  $\beta$  phase is not thermodynamically stable in any temperature range. The reason for the appearance of  $\beta$  phase is related to low interfacial tension of melt vs.  $\beta$ . It has been also shown that maximum crystallinity reached in experiments does not exceed 40–50% in agreement with the concept of constrained amorphous phase.

### Introduction

Basic equations of the model of phase transitions in a condensed three-phase system composed of one amorphous (liquid), and two polymorphic solid phases were derived in refs. [1, 2]. Two types of three-phase systems can be distinguished. In the first one (enantiotropic), all three phases are *stable* in some temperature range and, in a definite temperature, each pair of phases coexists in equilibrium. In the other (monotropic) type only two phases are stable and the third, *metastable* phase does not exist in equilibrium conditions. The monotropic system can be often met in polymers. In polymers crystalline fraction is often composed of two or more polymorphs, from which only one is thermodynamically stable, while those with higher free energy are metastable. Crystallization of long molecules is confined by a lot of barriers of various natures and the process of reaching equilibrium is much slower than that in low molecular weight materials. More than that, even in very long times crystallinity in polymers does not exceed some limit,  $x_{max} < 1$ . The reason for limited crystallinity of polymers based on constraints of the amorphous phase discussed in ref. [2] is perfectly consistent with our results. It is a characteristic of polymers that the actual phase composition is determined not only by the criterion of stability but also by the kinetics of formation of various polymorphs. If the rate of formation of a thermodynamically stable phase is low, crystallization will lead to formation of a polymorph with higher free enthalpy but with higher rate of formation (lower energetic barrier). There is an additional question if the metastable phase can

further transform into thermodynamically stable structure. According to the Ostwald step rule [3], transformation toward thermodynamic equilibrium occurs always via metastable states with increasing stability. Although there is no clear physical origin of this rule it is maintained that metastable states are realized because the local barrier of their formation is lower and local free enthalpy minimum can be reached faster than the global minimum in the equilibrium state. For instance the undercooled melt is per se a metastable state which on the way to the thermodynamic equilibrium needs to overcome a thermodynamic barrier related to the surface free energy. Another kinetic factor which can lead to simultaneous formation of two or more polymorphs can be related to molecular mobility. Crystallization of polymers is controlled not only by actual conditions ( $T$ ,  $p$ ) but also by the history of previous stages. This situation can result in formation of polymorphs, which are not thermodynamically stable but may exist for long times for kinetic reasons.

Cheng et al. [4, 5] discussed the problem of metastability and showed additional points related specifically to polymers. In the classical concepts of thermodynamics phases are assumed to be of infinite size. In practice, the characteristic size scale of phases in polymers is usually very small. Cheng et al. [4, 5] showed, using Gibbs-Thomson plot, that phases, stable at infinite size can be unstable at relatively small size. If the molecular mobility is very low, such phases may keep its structure for a long time. When the mobility is increased, a metastable phase may transform into the stable phase with different structure.

An example of a polymer with two solid polymorphs at atmospheric pressure is isotactic polypropylene. Crystallization from the melt leads to formation of stable  $\alpha$  phase usually accompanied by a small amount of  $\beta$  modification. Both forms have the same helix geometry but different chirality. In the case of  $\alpha$  crystals there are alternating left- and right hand helices while in  $\beta$  crystals all chains have the same helical hand, either left or right. There is opinion that one of the reasons for the formation of one form or another is related to molecular mobility, which in turn corresponds with the rate of crystallization [6, 7]. It is usually accepted that the  $\beta$  trigonal form is a metastable, intermediate on the way to the stable monoclinic  $\alpha$  modification. Under proper thermal treatment  $\beta$  form can be transformed into  $\alpha$  modification. An often raised question is what is the mechanism of the  $\beta \rightarrow \alpha$  transition. Polymorphic transitions can be generally divided into two categories – direct, usually cooperative solid – solid transitions and nucleation-controlled processes, sometimes involving partial melting and recrystallization. In polymers the solid-solid mechanism is usually applied to transitions in which molecular chains of mother and target phases have identical conformations or when the helical hands of molecular chains do not change during transition. In the case of polypropylene the mechanism often assumed is one involving partial melting and subsequent recrystallization, because of different arrangement of chain helical hands in  $\alpha$  and  $\beta$  crystals. Some experimental data obtained by DSC and WAXS [8-13] can indicate that the  $\beta \rightarrow \alpha$  transition occurs via amorphous phase, but direct experimental evidence is not available. Other authors claim that  $\beta \rightarrow \alpha$  transition in polypropylene occurs in a solid state. The essential role during this transition is played by propagation of conformational defects providing reversal of helical hand required by solid-solid transition [14]. Garbarczyk et al. [15, 16] maintain that there is no contradiction between both mechanisms. They have proposed [6] that mechanism of  $\beta \rightarrow \alpha$  transition is based on several types of chain movements; the phenomenon

identified by some authors as “melting” which can be interpreted as a translation of polymer chains perpendicular to their axes.

The aim of this paper is to elucidate the mechanism of phase transitions in isotactic polypropylene by experimental study and numerical simulation based on the nucleation-controlled model [1, 2].

## Results

WAXS analysis indicates that isothermal crystallization in the temperature range between 116 and 130 °C results in dominant formation of modification  $\alpha$  with some amount of modification  $\beta$ . In samples crystallized above 130 °C only  $\alpha$  modification is observed. Figure 1 illustrates WAXS profile obtained during isothermal crystallization at 123 °C.

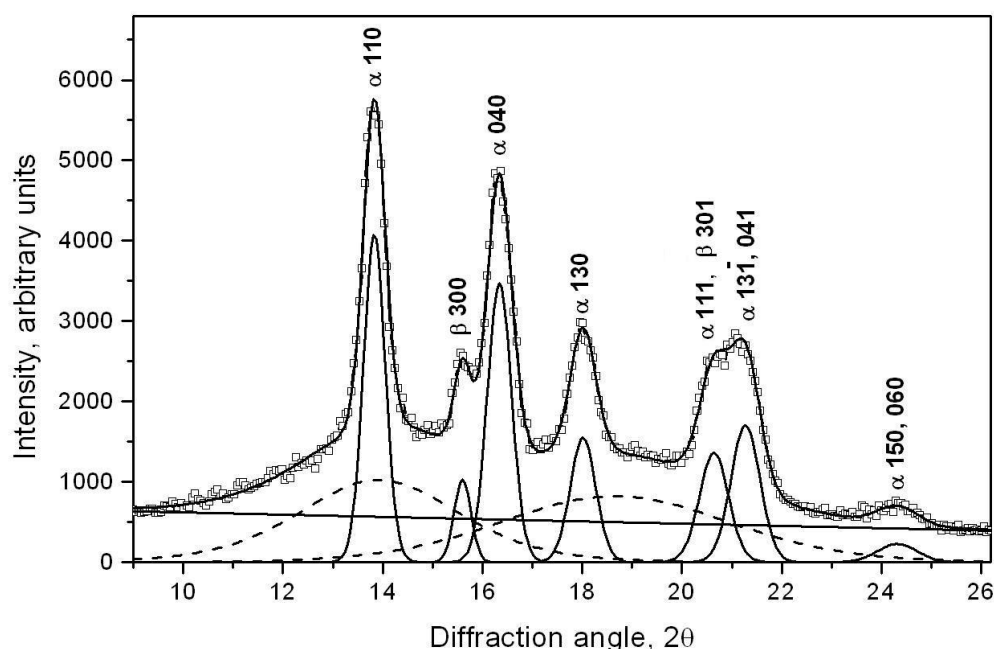
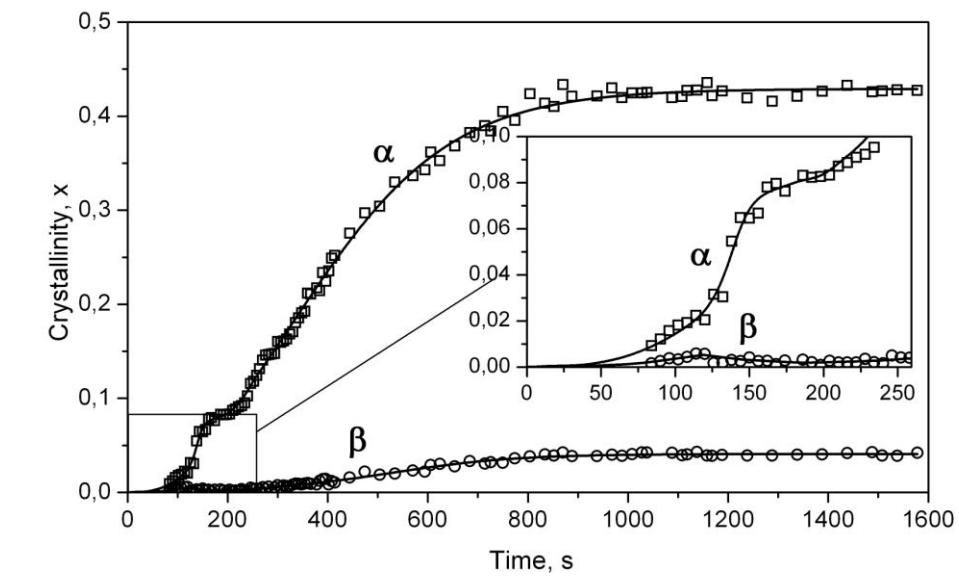


**Fig. 1.** WAXS profile of i-PP after 20 min of crystallization at 123 °C. Points - experimental data, solid lines - crystalline peaks, dashed lines - amorphous halo.

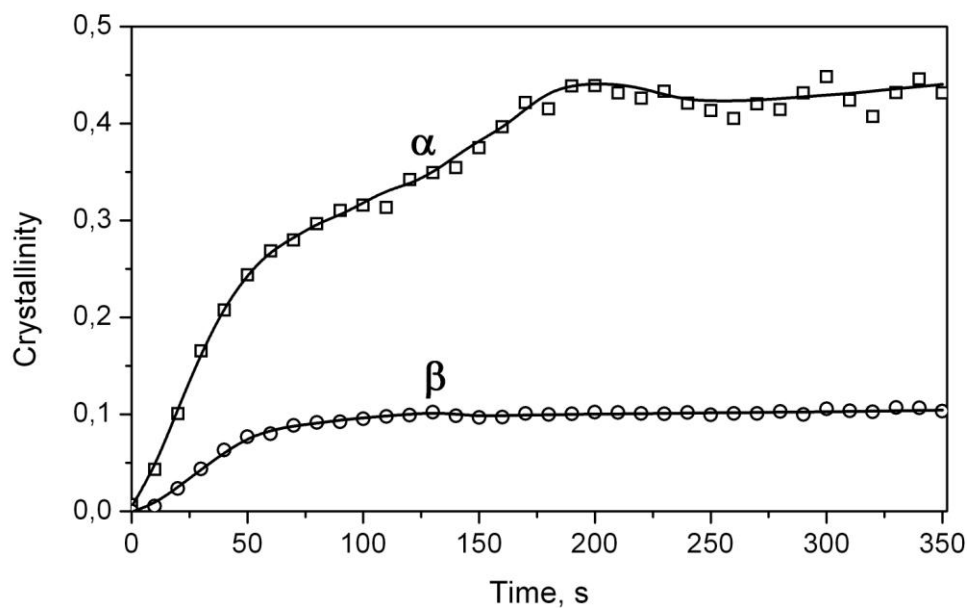
Fitting of experimental profiles results in several narrow peaks related to  $\alpha$  and  $\beta$  crystals and asymmetric amorphous halo. Asymmetric shape of the amorphous halo for i-PP was reported in [e.g.17]. This asymmetric shape was fitted with two Pearson VII peaks (Figure 1).

Figures 2 and 3 illustrate development of  $\alpha$  and  $\beta$  crystallinity during isothermal crystallization at 116 °C and 123 °C. Despite the fact that at particular temperature there is large scattering of data depending on the sample investigated, the general observation is that kinetic curves of formation of  $\alpha$  and  $\beta$  crystals cannot be described by sigmoidal function as it is usually found in simple crystallization involving single solid phase. The peculiar shapes of kinetic curves observed experimentally indicate a complex nature of phase transitions from amorphous phase. Some of the kinetic curves indicate a local maximum for  $\beta$  content followed by acceleration of  $\alpha$  formation

(Figure 2). The detailed look reveals that the amount of  $\beta$  modification in the early stages of the process is relatively high (up to 30%, Figure 3).



a)



b)

**Fig. 2.** Development of WAXS crystallinity during isothermal crystallization at 123 °C (a) and 116 °C (b).

At longer times the  $\beta/\alpha$  ratio is reduced which may suggest  $\beta'' \rightarrow \alpha$  transition. Quantitative analysis of the complex nature of phase transitions during isothermal crystallization will be described in a separate paper. In general, it is seen that isothermal transition processes in undercooled amorphous polypropylene extend

over hundreds of seconds. This suggests nucleation (diffusion) controlled mechanism in contrast to instantaneous, cooperative transitions between solid phases (e.g. martensite transitions).

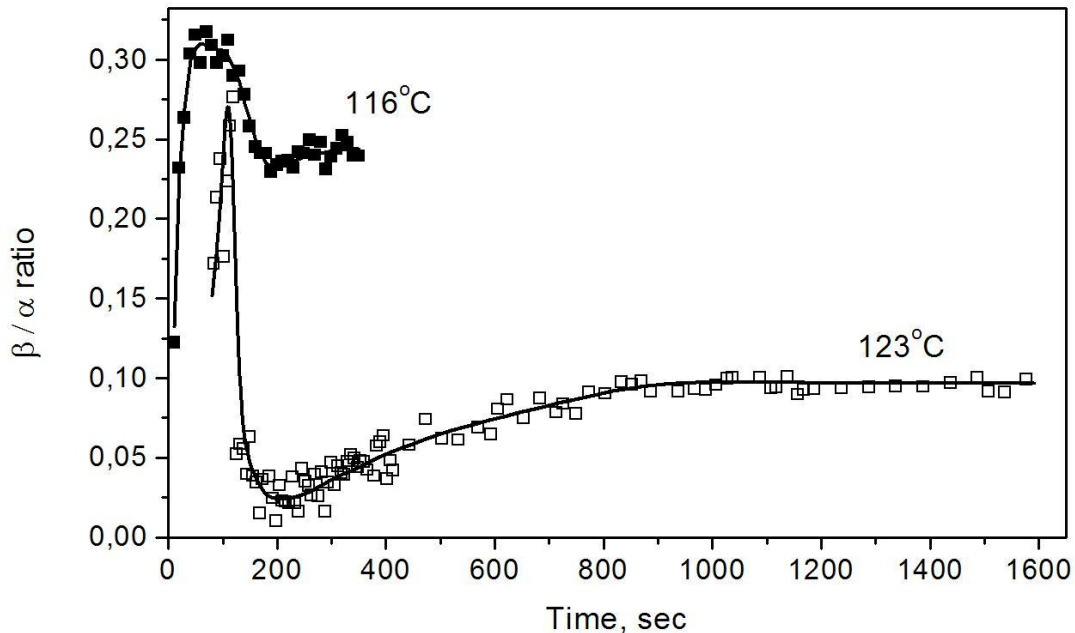


**Fig. 3.** Variation of the ratio of  $\beta$  to  $\alpha$  crystallinity during isothermal crystallization at  $116^\circ\text{C}$  and  $123^\circ\text{C}$ .

Polypropylene sample crystallized at  $123^\circ\text{C}$  and containing a mixture of  $\alpha$  and  $\beta$  crystals was subjected to heating at constant rate  $10\text{ K/min}$  (Figure 4). Reduction of crystalline contents starts at temperatures much lower than equilibrium melting temperatures of both phases,  $T_{\alpha,am}$ ,  $T_{\beta,am}$ , indicated in Table 1.  $\beta$  crystals disappear faster than  $\alpha$  crystals. Steep reduction of  $\beta$  crystallinity occurs in the temperature range of  $144 - 151^\circ\text{C}$  and that of  $\alpha$  crystals starts at  $147^\circ\text{C}$ . At the end of melting of  $\beta$  crystals ( $149^\circ\text{C}$ ), dynamics of  $\alpha$  crystallinity reduction becomes much slower and this trend is observed up to  $154^\circ\text{C}$ , being visible as plateau (Figure 4). This manifests formation of new  $\alpha$  crystals, which is superimposed on the melting of original  $\alpha$  crystals. It is very probable that the new  $\alpha$  crystals appear from  $\beta$  phase. The temperature delay of  $\alpha$  formation in relation to reduction of  $\beta$  crystallinity can be explained by transient effects in the kinetics of  $\beta \rightarrow \alpha$  transition. This kind of behavior was also observed by Garbarczyk et al [15]. Disappearance of  $\alpha$  crystals is observed around  $165^\circ\text{C}$ . For comparison, heating of the sample containing  $\alpha$  crystals only (Figure 5), shows continuous smooth reduction of crystallinity, as a result of melting, over wide range of temperatures. Complex character of transitions during heating is also evident in the light depolarization and differential scanning calorimetry (Figure 6). Crystallinity – temperature curves from WAXS and DSC measurements almost overlap. The depolarization characteristic  $DE(T)$  representing crystallinity and crystal thickness behaves in a way similar to WAXS and DSC.

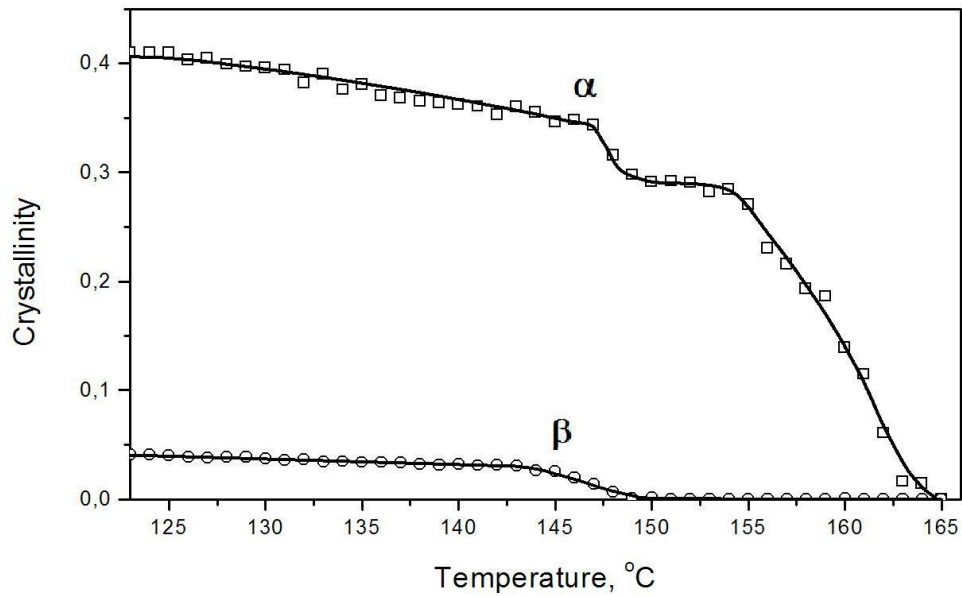


**Fig. 4.** Variation of WAXS crystallinity during heating at the rate of 10 K/min after isothermal crystallization at 123 °C (mixture  $\alpha+\beta$ ).

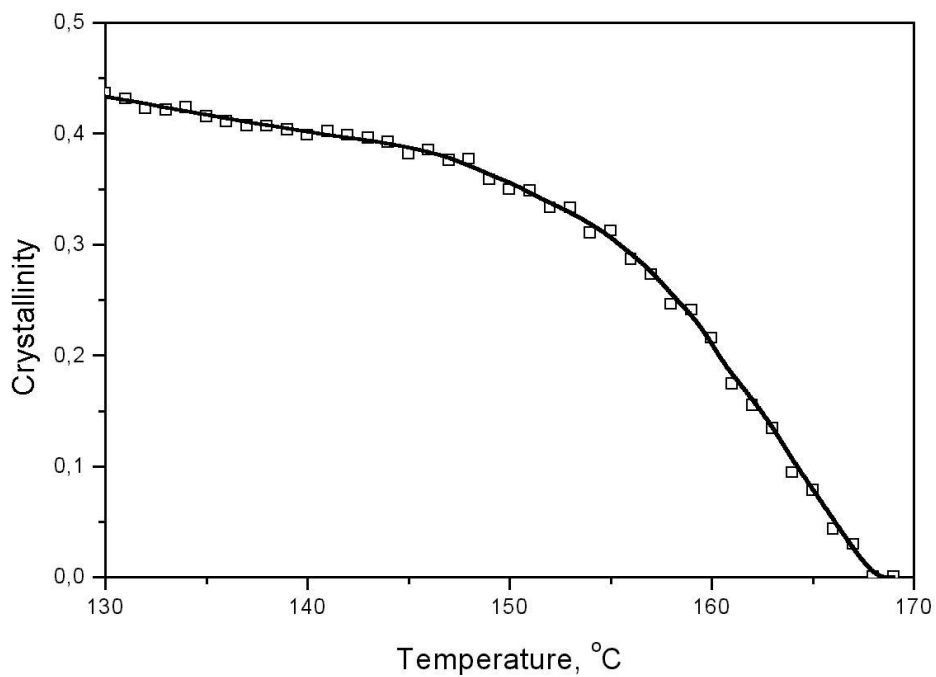


**Fig. 5.** Variation of WAXS crystallinity during heating at the rate of 10 K/min after isothermal crystallization at 130 °C (pure  $\alpha$  form).

Isothermal crystallization of undercooled amorphous sample (Figure 2) does not show melting of  $\beta$  crystals as an intermediate step of creation of the  $\alpha$  form. On the contrary, behavior of the  $\beta$  form contents with a local maximum and subsequent reduction supports direct, though not instantaneous, solid-solid transformation. In non-isothermal experiments (heating), however, there are conditions when  $\beta$  form is melted and the resulting amorphous phase is converted into  $\alpha$  crystals. It is evident in Figure 4 that formation of  $\alpha$  crystals (149 – 154 °C) as observed by WAXS is slightly delayed in the temperature scale with respect to melting of  $\beta$  crystals that is definitely finished at 152 °C.

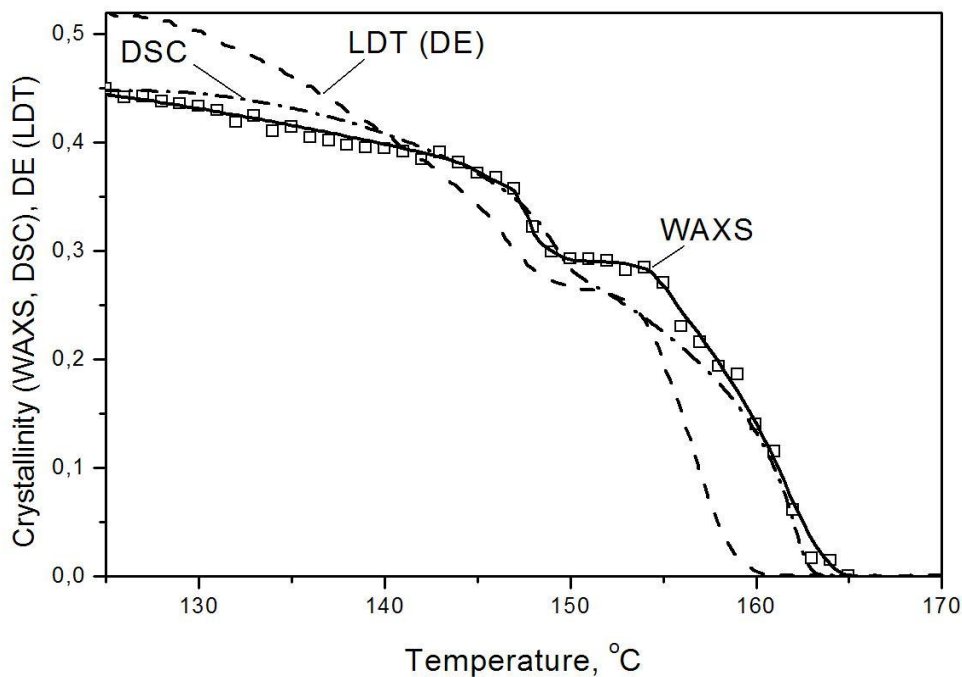


**Fig. 6.** Variation of total ( $\alpha + \beta$ ) crystallinity by WAXS, DSC and light depolarization technique (parameter DE) during heating of the crystalline sample at the rate of 10 K/min.

Figure 7 presents polarizing microscopic images taken at different temperatures during heating. It can be observed that main part of melting starts from highly birefringent  $\beta$  spherulites (151.5 °C), followed by formation of low-birefringence spherulites of the  $\alpha$  phase in the temperature range 152.0 °C - 152.5 °C. The last step consists in melting of  $\alpha$  spherulites, first those created from the  $\beta$  form (micrographs taken at 154.0 °C and 154.5 °C), and then (157.5 °C, 158.0 °C and 161 °C) original  $\alpha$  spherulites formed before heating.

The micrographs show melting of  $\beta$  phase followed by recrystallization in the  $\alpha$  form. So the non-isothermal polymorphic transition assumes the form  $\beta \rightarrow$  amorphous  $\rightarrow \alpha$ . This kind of transition is expected from the simulated phase diagram (Figure 8) in the temperature range  $190 < T < 210$  °C.

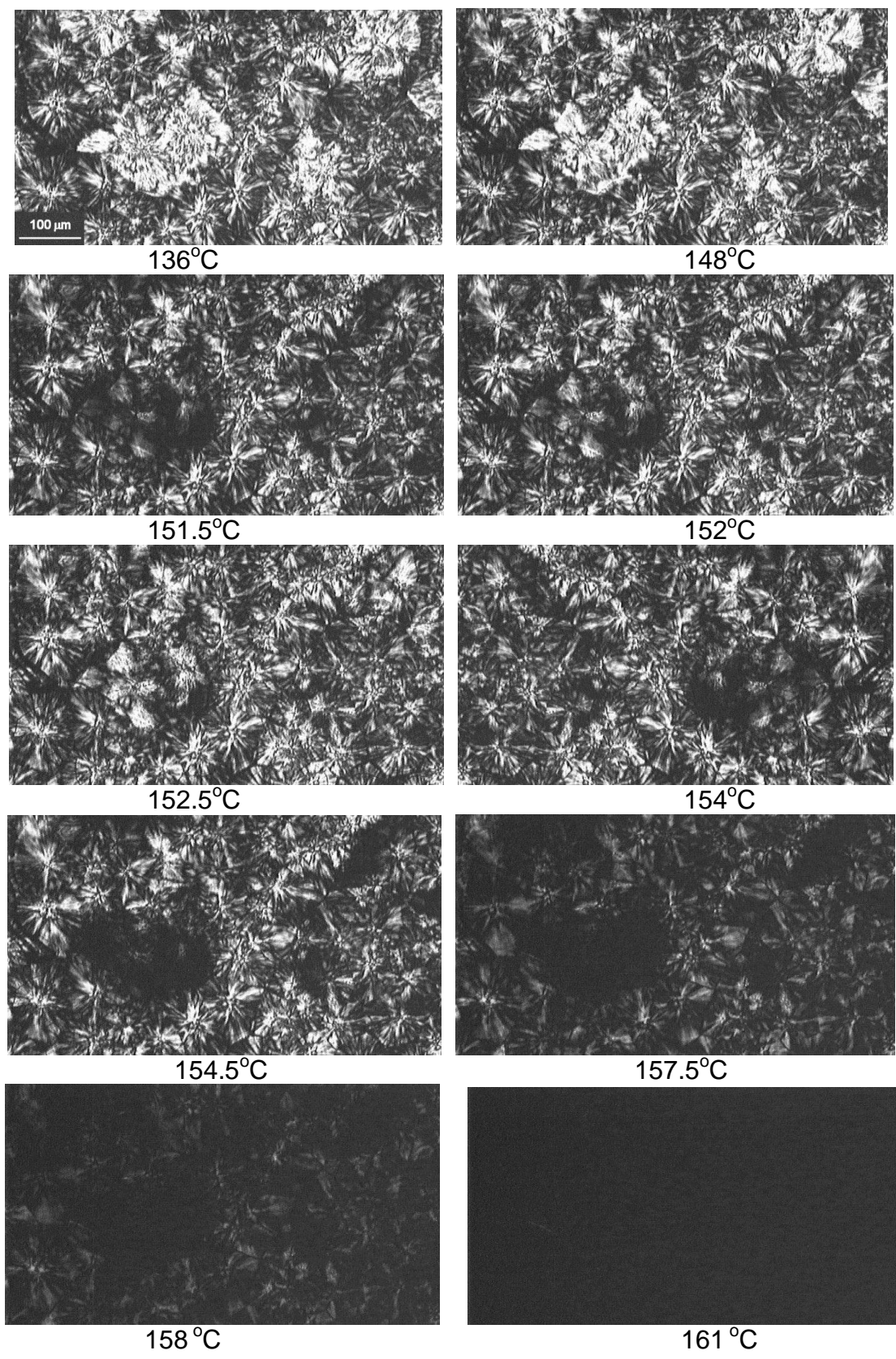


**Fig. 7.** The sequence of micrographs of crystalline polypropylene taken during heating at the rate 10 K/min (temperatures indicated).

### Numerical simulation of phase transitions

To analyze the problem of thermodynamic stability of the polypropylene  $\beta$  phase and mechanisms of polymorphic  $\alpha \leftrightarrow \beta$  transitions we have derived simplified isobaric phase diagram of the system. Assuming temperature-independent enthalpy and entropy, the plot of free enthalpy density for individual phases,  $g_{am}(T)$ ,  $g_{\beta}(T)$  and  $g_{\alpha}(T)$ , was obtained (Figure 8).

$$\begin{aligned}
 g_i(T) &= h_i - T s_i \\
 g_j(T) &= h_j - T s_j \\
 \Delta g_{ij}(T) &= g_j - g_i = \Delta h_{ij} - T \Delta s_{ij} \\
 \Delta g_{ij}(T_{ij}) &= 0 \\
 T_{ij} &= \frac{\Delta h_{ij}}{\Delta s_{ij}} = \frac{(\Delta h_{ik} - \Delta h_{jk}) T_{ik} T_{jk}}{\Delta h_{ik} T_{jk} + \Delta h_{jk} T_{ik}}
 \end{aligned} \tag{1}$$

Material characteristics used are collected in Table 1. Melting enthalpies,  $\Delta h_{i,am}$ , and melting temperatures,  $T_{i,am}$  of pure crystalline phases were taken from the literature [18]. The values of  $T_{i,am}$  and  $\Delta h_{i,am}$  found in the literature for both modifications are highly scattered. In general,  $T_{\alpha,am} > T_{\beta,am}$  and  $\Delta h_{\alpha,am} > \Delta h_{\beta,am}$ . The thermodynamic characteristics for polymorphic transitions  $\beta \leftrightarrow \alpha$  were estimated from the principle of additivity.

$$\begin{aligned}
 \Delta g_{ij} &= \Delta g_{ik} - \Delta g_{jk} \\
 \Delta h_{ij} &= \Delta h_{ik} - \Delta h_{jk} \\
 \Delta s_{ij} &= \Delta s_{ik} - \Delta s_{jk}
 \end{aligned} \tag{2}$$

It is evident in Figure 8 that phase  $\beta$  is thermodynamically unstable. There is no temperature in which  $\beta$  form would exhibit minimum free enthalpy. Stable phases include low-temperature solid form  $\alpha$  in the temperature range below  $T_{\alpha,am}$ , and amorphous phase above this temperature. Phase diagram consisting of two stable and one unstable phase (Figure 8) is typical for monotropic systems. The presence of metastable  $\beta$  phase has been made evident in our experiments.

Activation energy,  $E_D$  within the amorphous phase was taken from the literature as energy of self-diffusion. The literature offers different  $E_D$  values in amorphous polypropylene, ranging from 40 [19] to 89 kJ/mol [20]. Activation energy for motions within the solid phases can be expected to be much higher than those for the melt, but no direct experimental evidence is available. To estimate other material characteristics unavailable from the literature, empirical correlations have been used.

The unknown value of side surface tension of  $\beta$  crystals vs. melt, was calculated from that of  $\alpha$  crystals using the Turnbull formula [21]

$$\frac{\sigma_{am,\beta}^s}{\sigma_{am,\alpha}^s} \cong \left| \frac{\Delta h_{am,\beta}}{\Delta h_{am,\alpha}} \right| \tag{3}$$

Interface tension between two polymorphic (solid) phases was obtained from the Antonoff approximation [22]

$$\sigma_{\alpha,\beta} \cong |\sigma_{\alpha} - \sigma_{\beta}| \quad (4)$$

The average interface tension between phases “*i*” and “*j*” were defined as

$$\bar{\sigma}_{ij} = [\sigma_{ij}^e (\sigma_{ij}^s)^2]^{1/3} \quad (5)$$

where the superscript “*e*” denotes chain-folded crystal face normal to polymer chain, and “*s*” – side face parallel to polymer chains.

The kinetics of phase transitions in a three-phase system composed of amorphous and two polymorphic solid phases were described with the use of the model of nucleation-controlled transitions in multi-phase systems [1, 2]. The model provides an extended version of the original probabilistic model of Kolmogoroff [27], Avrami [28], Johnson & Mehl [29] and Evans [30] and its multicomponent version [1].

According to ref. [2], amorphous phase “*am*” is divided into two different fractions: unconstrained, crystallizable fraction “*un*” and constrained fraction “*con*” which does not participate in crystallization and melting processes.

$$x_{am}(t) = x_{un}(t) + x_{con}(t)$$

$$x_{un}(t) = x_{max} - x_{\beta}(t) - x_{\alpha}(t) \quad (6)$$

$$x_{con}(t) = x_{con}^0 = 1 - x_{max}$$

$x_{max}$  - maximum crystallinity - is assumed a constant parameter characterizing constraints in the amorphous phase.

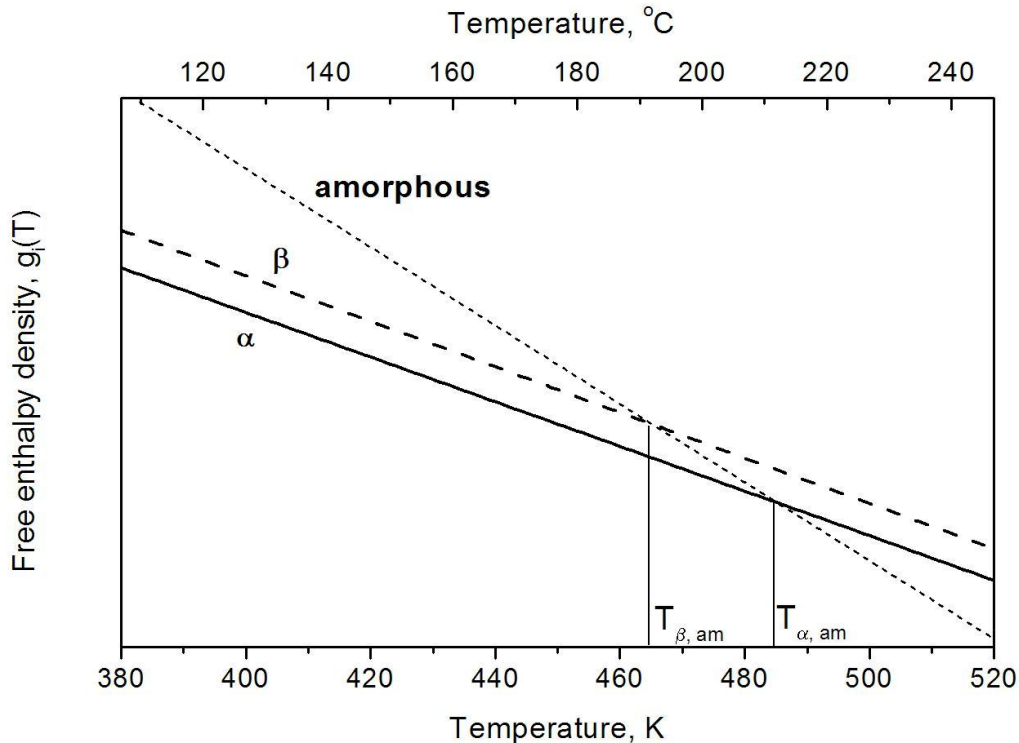


**Fig. 8.** Simulated isobaric phase diagram for isotactic polypropylene.

**Tab. 1.** Material characteristics in numerical simulation of phase transitions in i-PP.

Parameter, unit	Description	Value	Source
$T_{\beta,am}$ , K	Melting temperature of $\beta$	465.2	[18]
$T_{\alpha,am}$ , K	Melting temperature of $\alpha$	485.2	[18]
$T_{\beta,\alpha}$ , K	Transition temperature $\beta \rightarrow \alpha$	1219.3	Eqs. (2)
$\Delta h_{\beta,am}$ J/g	Melting enthalpy of $\beta$	194.9	[18]
$\Delta h_{\alpha,am}$ J/g	Melting enthalpy of $\alpha$	208.8	[18]
$\Delta h_{\beta\alpha}$ J/g	Transition enthalpy $\beta \rightarrow \alpha$	13.9	Eqs. (2)
$\Delta s_{\beta,am}$ J/g K	Melting entropy of $\beta$	0.4179	Eqs. (2)
$\Delta s_{\alpha,am}$ J/g K	Melting entropy of $\alpha$	0.4303	Eqs. (2)
$\Delta s_{\beta\alpha}$ J/g K	Transition entropy $\beta \rightarrow \alpha$	0.0114	Eqs. (2)
$E_D^{am}$ , kJ/mol	Activation energy of molecular motions, amorphous phase	70.5	fitted
$E_D^\beta$ , kJ/mol	Activation energy of molecular motions, $\alpha$ and $\beta$ phases	106.5	fitted
$E_D^\alpha$ , kJ/mol			
$\sigma_{\beta,am}^e$ , erg/cm <sup>2</sup>	Interface tension $\beta$ vs. melt, chain-folded face	50	[23]
$\sigma_{\alpha,am}^e$ , erg/cm <sup>2</sup>	Interface tension $\alpha$ vs. melt, chain-folded face	122	[24]
$\sigma_{\alpha,\beta}^e$ , erg/cm <sup>2</sup>	Interface tension $\beta$ vs. $\alpha$ , chain-folded face	72	Eq. (4)
$\sigma_{\beta,am}^s$ , erg/cm <sup>2</sup>	Interface tension $\beta$ vs. melt, side face	10.4	Eq. (3)
$\sigma_{\alpha,am}^s$ , erg/cm <sup>2</sup>	Interface tension $\alpha$ vs. melt, side face	11.5	[25]
$\sigma_{\alpha,\beta}^s$ , erg/cm <sup>2</sup>	Interface tension $\beta$ vs. $\alpha$ , side face	1.1	Eq.(4)
$\bar{\sigma}_{\beta,am}$ , erg/cm <sup>2</sup>	Average interface tension $\beta$ vs. melt	17.553	Eq.(5)
$\bar{\sigma}_{\alpha,am}$ , erg/cm <sup>2</sup>	Average interface tension $\alpha$ vs. melt	25.269	Eq. (5)
$\bar{\sigma}_{\alpha,\beta}$ , erg/cm <sup>2</sup>	Average surface tension $\beta$ vs. $\alpha$	4.433	Eq.(5)
$v_0$ , nm <sup>3</sup>	Volume of a kinetic element	0.1968	calculated
$\rho_{am}$ , g/cm <sup>3</sup>	Amorphous density	0.854	[26]
$\rho_\beta$ , g/cm <sup>3</sup>	Density of $\beta$	0.939	[26]
$\rho_\alpha$ , g/cm <sup>3</sup>	Density of $\alpha$	0.949	[26]
$X_{max}$	Maximum crystallinity	0.45 – 0.47	fitted

According to the phase diagram (Figure 8), in the temperatures  $T < T_{m,\beta}$ , i.e. below melting temperature of both solid phases, three thermodynamically transitions are possible: direct crystallization of the unconstrained amorphous phase into the  $\beta$  phase, “un”  $\rightarrow$  “ $\beta$ ”, direct crystallization of the amorphous phase into the  $\alpha$  phase, “un”  $\rightarrow$  “ $\alpha$ ”, and polymorphic transition “ $\beta$ ”  $\rightarrow$  “ $\alpha$ ”. There is no thermodynamic background for melting phase “ $\beta$ ” on the way to phase “ $\alpha$ ”. Consider isothermal development of phase structure in a pure undercooled amorphous phase at  $T < T_{\beta,am}$ . After time,  $t$ , the phase composition reads

$$\begin{pmatrix} x_{am}^0 = 1 \\ x_{\beta}^0 = 0 \\ x_{\alpha}^0 = 0 \end{pmatrix} \xrightarrow{E_{ij}(t)} \begin{pmatrix} \frac{1 - x_{\max} + x_{\max} e^{-E_{am,\beta} - E_{am,\alpha}}}{E_{\beta,\alpha} - E_{am,\beta} - E_{am,\alpha}} \left( \frac{x_{\max} E_{am,\beta}}{E_{\beta,\alpha} - E_{am,\beta} - E_{am,\alpha}} (e^{-E_{am,\beta} - E_{am,\alpha}} - e^{-E_{\beta,\alpha}}) \right) \\ \frac{x_{\max}}{E_{\beta,\alpha} - E_{am,\beta} - E_{am,\alpha}} \left[ (E_{\beta,\alpha} - E_{am,\alpha})(1 - e^{-E_{am,\beta} - E_{am,\alpha}}) - E_{am,\beta}(1 - e^{-E_{\beta,\alpha}}) \right] \end{pmatrix} \quad (7)$$

where functions  $E_{ij}(t)$  represent progress of individual transitions up to time  $t$  and are related to transition rates  $K_{ij}$  derived from the classical nucleation theory.

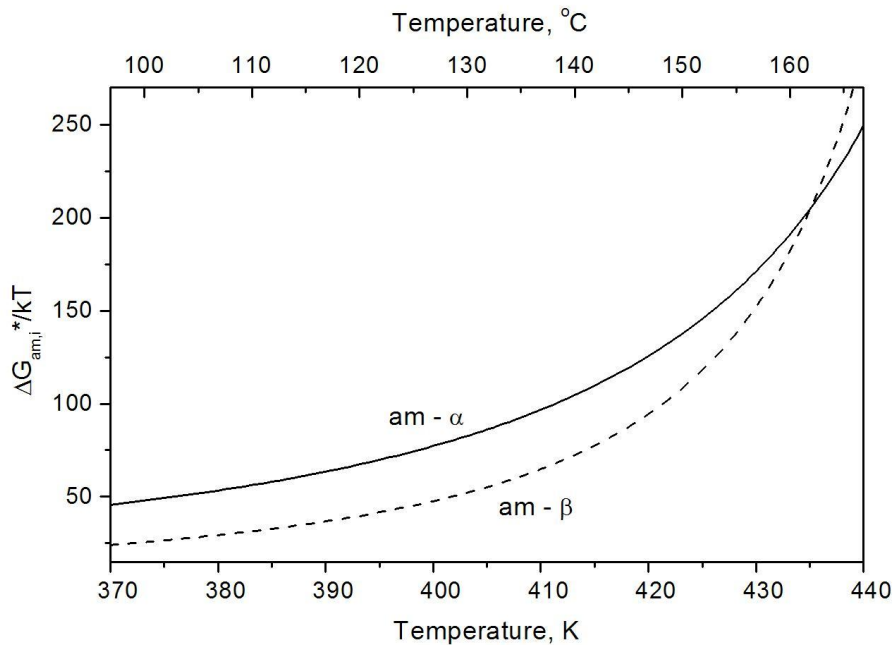


**Fig. 9.** Potential barriers  $\Delta G_{am,i}^*/kT$  calculated for primary nucleation of  $\alpha$  and  $\beta$  polypropylene crystals from amorphous phase. Material characteristics are taken from Table 1.

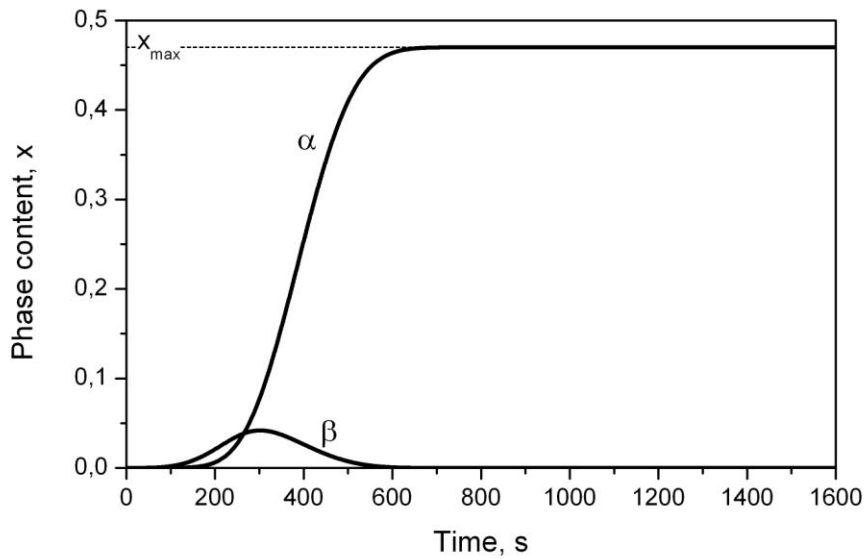


**Fig. 10.** Numerical simulation of isothermal crystallization (based on sporadic nucleation) of undercooled amorphous polypropylene at 123 °C. Material characteristics are from Table1.

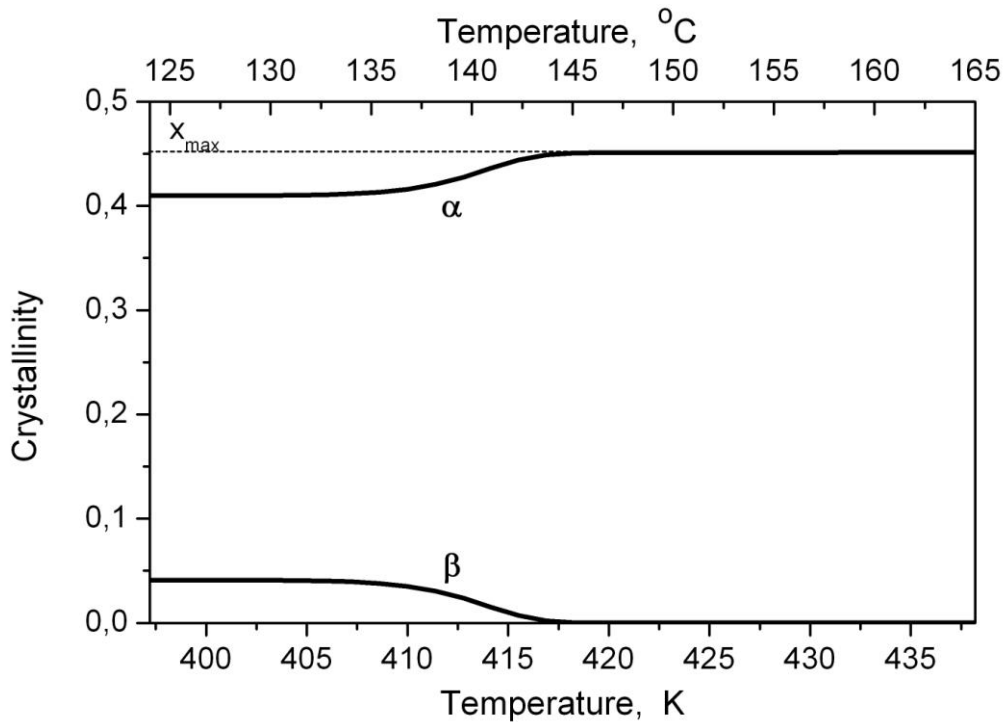


**Fig. 11.** Numerical simulation of heating at 10 K/min of crystalline polypropylene (sporadic nucleation, material characteristics are from Table 1).

Thermodynamically admissible transitions below melting temperature of phase  $\beta$  include simultaneous crystallization of the unconstrained amorphous phase into solid phases “ $\beta$ ” and “ $\alpha$ ”, and direct polymorphic transition “ $\beta$ ”  $\rightarrow$  “ $\alpha$ ”. In the temperatures studied experimentally (116 °C and 123 °C) the model does not predict melting of phase “ $\beta$ ”.

In the range of very short times ( $=$  small  $E_{ij}$ ) Eq. (7) reduces to

$$\begin{pmatrix} x_{am}^0 \\ x_{\beta}^0 \\ x_{\alpha}^0 \end{pmatrix} \xrightarrow{E_{ij}(t) \ll 1} \begin{pmatrix} 1 - x_{max}(E_{am,\beta} + E_{am,\alpha}) \\ x_{max} E_{am,\beta} \\ x_{max} E_{am,\alpha} \end{pmatrix} \quad (8)$$

It should be noted that Eq. (8) does not depend on the kinetic characteristic  $E_{\beta\alpha}$ , describing direct polymorphic transition “ $\beta$ ” $\rightarrow$  “ $\alpha$ ”.

For sporadic, isothermal nucleation, transition rate function is controlled by two factors: molecular mobility within the source phase (here: “ $am$ ”) characterized by activation energy,  $E_D$ , and thermodynamic barrier of nucleation,  $\Delta G^*$

$$\begin{aligned} E_{am,\beta}(t) &\propto e^{-\frac{E_D^{am,\beta}}{kT}} e^{-\frac{\Delta G_{un,\beta}^*}{kT}} t^4 \\ E_{am,\alpha}(t) &\propto e^{-\frac{E_D^{am,\alpha}}{kT}} e^{-\frac{\Delta G_{un,\alpha}^*}{kT}} t^4 \\ E_D^{am,\beta} &= E_D^{am,\alpha} = E_D^{am} \\ \frac{E_{am,\beta}(t)}{E_{am,\alpha}(t)} &\cong \exp \left[ \frac{1}{kT} (\Delta G_{am,\alpha}^* - \Delta G_{am,\beta}^*) \right] \\ \Delta G_{am,i}^* &= \frac{32 \bar{\sigma}_{am,i}^3}{\Delta g_{am,i}^2} \end{aligned} \quad (9)$$

where  $E_D^{am}$  is activation energy for molecular motions in the unconstrained amorphous phase,  $\Delta g_{am,\beta}$  and  $\Delta g_{am,\alpha}$  are bulk free enthalpy densities per unit mass and  $\bar{\sigma}_{am,\beta}$ ,  $\bar{\sigma}_{am,\alpha}$  - average interface tensions, between the amorphous phase on one side and solid phases  $\beta$  and  $\alpha$  on the other one.

Putting in Eq. (8)

$$\begin{aligned} \Delta G_{am,\alpha}^* &\gg \Delta G_{am,\beta}^* \\ E_{am,\alpha} &\ll E_{am,\beta} \ll 1 \end{aligned} \quad (10)$$

one obtains locally (near start of the transition) relatively high concentration of  $\beta$  phase. Figure 9 presents reduced potential barriers  $\Delta G_{am,i}^*/kT$  for the transitions “ $un$ ” $\rightarrow$  “ $\alpha$ ” and “ $un$ ” $\rightarrow$  “ $\beta$ ”. It is evident that below 162 °C the thermodynamic barrier for nucleation of phase  $\alpha$  is higher than that for phase  $\beta$ , the controlling factor being interface tension:

$$\frac{\sigma_{am,\alpha}^3}{\Delta h_{am,\alpha}^2} > \frac{\sigma_{am,\beta}^3}{\Delta h_{am,\beta}^2} \quad (11)$$

At longer times, phase  $\beta$  is accumulated and polymorphic transition “ $\beta$ ” $\rightarrow$  “ $\alpha$ ” switches on, Concentration of phase  $\beta$  passes through a maximum, decreases and

the instantaneous composition reaches the form indicated in Eq. (7). At long times as soon as crystallizable (unconstrained) amorphous phase, “un”, is exhausted, phase composition is controlled solely by the progress of the  $\beta \rightarrow \alpha$  polymorphic transition

$$\begin{pmatrix} x_{am}^0 \\ x_{\beta}^0 \\ x_{\alpha}^0 \end{pmatrix} \xrightarrow{E_{ij}(t) \gg 1} \begin{pmatrix} 1 - x_{max} \\ e^{-E_{\beta,\alpha}} \\ x_{max} (1 - e^{-E_{\beta,\alpha}}) \end{pmatrix} \xrightarrow{E_{ij}(t) \rightarrow \infty} \begin{pmatrix} 1 - x_{max} \\ 0 \\ x_{max} \end{pmatrix} \quad (12)$$

Asymptotically, fraction of thermodynamically stable phase “ $\alpha$ ” reaches the maximum available level  $x_{max}$  and is accompanied by constrained (uncrystallizable) amorphous phase

Figure 10 presents simulation of isothermal crystallization of undercooled amorphous polypropylene at 123 °C and Figure 11 – simulation of slow (quasi-static) heating of crystalline polypropylene.

Some features observed in the crystallization experiment (Figure 2) are consistent with simulation (Figure 10). Both in experiment and simulation, formation of  $\beta$  and  $\alpha$  phases starts simultaneously around 100 s and fraction of the target phase  $\alpha$  asymptotically approaches the limit  $x_{max}$ . Experimental behavior of the  $\beta$  phase, however, differs from that predicted in simulation. In the experiments,  $\beta$  phase fraction approaches 0.04 to 0.1 and remains constant up to the end of the experiment while simulation predicts maximum of  $\beta$  followed by complete disappearance of  $\beta$  in times longer than 550 s. Discrepancy between experimental and simulated behavior may be due to the uncertainty of the material characteristics assumed.

Considerably different is experimentally observed and simulated behavior in heating (Figure 4 vs. Figure 11). Experiments (Figure 4) show reduction of  $\alpha$  and  $\beta$  crystallinity, starting around  $T = 125$  °C and finished at 149 °C ( $\beta$  form) and 165 °C ( $\alpha$  form), i.e. well below equilibrium melting temperatures  $T_{\beta,am}$  and  $T_{\alpha,am}$ . This is as a consequence of melting being predominant over  $\beta \rightarrow \alpha$  transition. On the other hand, simulation (Figure 11) indicates nearly constant fractions of solid phases up to 133 °C, and  $\beta \rightarrow \alpha$  transition in the range of 133 – 145 °C followed by disappearance of the  $\beta$  form and leveling off phase  $\alpha$  at the level  $x_{max}$ . No melting of phase  $\alpha$  up to 165 °C is predicted.

## Discussion

Experiments and numerical simulation provide information about several aspects of polypropylene crystallization involving polymorphic phases  $\beta$  and  $\alpha$ . Time scale of crystallization processes (hundreds of seconds) suggests nucleation-controlled mechanism of all transitions. Neither primary crystallization of the amorphous phase nor polymorphic transitions or melting, do resemble instantaneous, cooperative transitions observed in some materials (e.g. martensitic transitions).

Metastability of phase  $\beta$  is evident in the simulated phase diagram (Figure 8). In contrast to the stable phase  $\alpha$ , there are no conditions in which phase  $\beta$  would exist in equilibrium. Simulated isothermal kinetics (Figure 10) shows disappearance of phase  $\beta$  as a result of polymorphic transition into the stable phase  $\alpha$ . In isothermal crystallization experiments (Figure 2) concentration of  $\beta$  phase does not drop to zero as expected but exists in the system up to the end of the experiment. A possible

explanation of this discrepancy is activation energy for molecular motions, higher than assumed in the model and possibly growing in time. An increase of crystallinity combined with increase of activation energy may lead to slowing down of the transitions.

The mechanism of polymorphic transition is referred to phase diagram, Figure 8. Below melting temperature of the  $\beta$  phase (192 °C), thermodynamic condition of melting  $\beta$  is not satisfied. The experimentally observed isothermal  $\beta \rightarrow \alpha$  transition in low-temperatures (116 and 123 °C) can only be interpreted as a direct, non-cooperative polymorphic transition. In higher temperatures melting of  $\beta$  crystals is thermodynamically possible. Microscopic observations (Figure 7) provide an evidence of melting of  $\beta$  spherulites followed by recrystallization to  $\alpha$  spherulites.

Continuous reduction of  $\alpha$  and  $\beta$  crystallinity observed experimentally (Figures 4 and 5) and their disappearance at temperatures much lower than predicted from equilibrium characteristics (observed melting range 150-170 °C, predicted  $T_{\beta,am} = 192$  °C,  $T_{\alpha,am} = 209$  °C) suggests that crystalline phases consist of small, defective units distributed with respect to size and degree of perfection. The first crystallites which melt at lowest temperatures are those which are the smallest and/or most defective. Simulation model assuming three ideal, well defined phases (Figures 8 and 11) is incapable of describing the observed non-isothermal behavior of polypropylene. More complex model, admitting a distribution of crystalline structure would be welcome.

## Conclusions

Isothermal crystallization and heating of isotactic polypropylene was followed with wide-angle X-ray scattering, calorimetry, optical microscopy and light depolarization technique. At normal pressure three phases were identified: amorphous phase, monoclinic crystalline phase  $\alpha$  and trigonal crystalline phase  $\beta$ . The simulated three-phase system (Figure 8) suggests that  $\beta$  polymorph is metastable and in no temperature does appear in equilibrium. Consequently, the system should be classified as monotropic.  $\beta$  phase appears in low temperatures as an intermediate between amorphous phase and stable crystalline phase  $\alpha$ . The nature of temporary appearance of the  $\beta$  polymorph is kinetic. Low interface tension and low potential barrier of nucleation of  $\beta$  crystals (cf. Figure 9 and Eqs. 10, 11) leads to high  $\beta$ -nucleation rate, compared with that of phase  $\alpha$ . At the start of crystallization, phases  $\alpha$  and  $\beta$  are created directly from the amorphous phase. In longer times, phase  $\beta$  is converted into the stable  $\alpha$  form. In contrast to instantaneous cooperative (martensite-like) transitions, polymorphic solid-solid transition  $\beta \rightarrow \alpha$  is nucleation-controlled.

Simple kinetic model developed in refs. [1, 2] allows to understand some features of phase transitions. Limited crystallinity is consistent with the concept of constrained amorphous phase [2]. The kinetics of isothermal formation and disappearance of the metastable solid polymorph  $\beta$  agree qualitatively with experimental evidence.

There are several discrepancies between experimental results and model predictions. The model requires that in low temperatures metastable  $\beta$  form is gradually, but completely converted into the stable  $\alpha$  modification. Within the duration of WAXS measurements (i.e. up to 1600 s)  $\beta$  crystals do not disappear completely. Heating of crystalline samples demonstrates reduction of the amount of both solid phases distributed over temperature range 125 – 165 °C i.e. well below equilibrium

melting temperatures predicted from the phase diagram, Figure 8 (192 and 209 °C). This suggests that crystalline phases consist of small, defective units distributed with respect to size and degree of perfection. The units which melt at low temperatures are small and/or most defective.

It is evident that our three-phase model assuming constant enthalpy and entropy is too simplified to be applied to crystallization of polypropylene. Better correspondence between the model and experimental results might be achieved by introduction of crystallinity-dependent parameters (such as activation energy of molecular mobility,  $E_D$ ), a distribution of crystal sizes, and/or different values of the Avrami exponent  $n$ .

## Experimental part

### Materials

Isotactic polypropylene (i-PP) (Himont),  $M_W = 476$  kDa,  $M_n = 79$  kDa, isotacticity index 0.96, was investigated. Polymer films were compression molded at 190°C for 10 min in a laboratory press.

### Methods

Isothermal crystallization of i-PP films was investigated in the temperature range between 116 and 130 °C. Isothermal crystallization was preceded by melting at 190 °C for 10 minutes followed by relatively fast cooling to desired crystallization temperature. According to our experience application of low melting temperature enables formation of relatively high content of  $\beta$  modification in pure i-PP. After isothermal crystallization, phase changes during heating from isothermal step were investigated.

Kinetics of phase transitions during isothermal crystallization and heating were investigated using wide-angle X-ray scattering (WAXS), light depolarization technique (LDT), DSC and optical microscopy (OM). Numerical simulation was performed using the model described in refs. [1, 2].

### Wide-angle X-ray scattering

Wide-angle X-ray scattering (WAXS) experiments were performed at the Soft Condensed Matter Beamline A2 at the Hamburg Synchrotron Radiation Laboratory (HASYLAB) at the German Electron Synchrotron (DESY) in Hamburg. The monochromatic radiation of wavelength,  $\lambda = 0.15$  nm was used. One-dimensional detector covering the angular range  $2\theta$  between 9 and 27° was used. The time of registration was usually between 5 and 11 seconds. The primary beam intensity was measured by an ionization chamber and the scattering intensity was normalized by dividing by the intensity of primary beam. The spatial calibration was done using PET film. The intensity normalization was performed using the Otoko software.

WAXS measurements were used for determination of the actual  $\alpha$  and  $\beta$  crystallinity. The WAXS scattering intensity was corrected by subtracting the background intensity. WAXS profiles were subjected to deconvolution technique using Pearson-VII function for all peaks. Taking into account possible formation of two polymorphs,  $\alpha$  and  $\beta$  contents were determined separately. The reliable determination of  $\alpha$  and  $\beta$  crystallinities needs separation of (111)  $\alpha$  and (301)  $\beta$  peaks both appearing at the angle  $2\theta = 20.6^\circ$  (the values of diffraction angle given for elevated temperatures of

isothermal crystallization, see Figure 1). In order to do this, we have estimated the ratio of the intensity of (111)  $\alpha$  reflection to the neighboring peak at  $2\theta = 21.3^\circ$  corresponding to the planes  $(13\bar{1})$  and (041) of  $\alpha$  modification, using i-PP with only  $\alpha$  modification as being equal to 0.57. The excess of intensity of the peak at  $2\theta = 20.6^\circ$  above the ratio of 0.57 in relation to the intensity of the  $\alpha$  peak at  $2\theta = 21.3^\circ$  was ascribed to  $\beta$  modification. The  $\alpha$  and  $\beta$  crystallinity was determined using areas of the respective peaks:

$$x_\alpha = \left( A_{(110)\alpha} + A_{(040)\alpha} + A_{(130)\alpha} + 1.57 \cdot A_{(13\bar{1})\alpha(041)\alpha} + A_{(150)\alpha(060)\alpha} \right) / A_{tot} \quad (13)$$

$$x_\beta = \left( A_{(300)\beta} + A_{(111)\alpha(301)\beta} - 0.57 \cdot A_{(13\bar{1})\alpha(041)\alpha} \right) / A_{tot} \quad (14)$$

The value of  $A_{tot}$  represents total area of all peaks, crystalline and amorphous recorded up to the scattering angle,  $2\theta = 27^\circ$ .

### Light depolarization technique (LDT)

Light depolarization measurements were done using the setup described in ref. [31]. Linearly polarized light was passed through the sample and then divided into two beams. One of the beams passes an analyzer (with optical axis perpendicular to that of the polarizer) and recorded with detector 1, the other beam is directed to detector 2 without change of polarization. Depolarization ratio was recorded directly. The source of light was He-Ne laser (5 mW) with wavelength  $\lambda = 633$  nm. Early papers introducing light depolarization assumed depolarization ratio,  $J$ , as directly proportional to the degree of crystallinity,  $x$  [32-34]. More recent analysis [35] has shown that depolarization ratio is a non-linear function of crystallinity and dimensions of depolarizing units determines crystallization parameter,  $DE$ :

$$J = 1 - e^{-DE} = DE + \frac{1}{2} (DE)^2 + \dots \quad (15)$$

where  $D$  is optical retardation of a single crystalline unit

$$D = \sin^2 \left( \frac{\pi \Delta n d}{\lambda} \right) \quad (16)$$

and  $E$  is average number of crystal plates in the path of the light beam

$$E = \frac{N f}{F} = \frac{x B}{d} \quad (17)$$

where  $F$  and  $B$  are, respectively, surface area and thickness of the sample, and  $f$  and  $d$  are average dimensions of a single crystal plate. Assuming thin, narrowly distributed crystal plates,  $DE$  appears to be proportional to the degree of crystallinity,  $x$ , multiplied by plate thickness,  $d$

$$D \cong \left( \frac{\pi \Delta n d}{\lambda} \right)^2 \quad (18)$$

$$DE = \ln \left[ \frac{1}{1 - J} \right] \propto (x \cdot d)$$

In the process of crystallization involving one crystal phase only, depolarization ratio and the parameter  $DE$  change with time or temperature in a smooth way. In a sample containing two different kinds of crystal plates, however

$$DE \cong C_i x_i d_i + C_j x_j d_j \quad (19)$$

Consequently, kinks or inflections of the temperature dependence of the parameter  $DE$  may suggest melting or polymorphic transitions of individual phases.

### *Polarizing microscopy*

The polarization-interference microscope MPI-5 produced by Polish Optical Works (PZO) and equipped with a temperature controllable oven was used. The microscope was operated with crossed polaroids with optional Wollastone prism. The images were recorded with a CCD camera and transmitted in a digital mode to the computer. Polymer films have been inserted between microscope glasses separated by mica spacers (30  $\mu\text{m}$  thick).

### *Differential scanning calorimetry (DSC)*

The DSC Perkin-Elmer Pyris-1 was used for isothermal crystallization followed by heating. Standard calibration was performed using indium and zinc. Samples were purified with nitrogen.

### *Acknowledgements*

This work was supported by the Polish Ministry of Science and Higher Education under Grant N507 019 31/0563. WAXS and SAXS experiments were carried out at the Hamburg Synchrotron Radiation Laboratory (HASYLAB) at the German Electron Synchrotron (DESY) in Hamburg in the frame of I-20070027 EC project. The research leading to these results has received funding from the European Community's Seventh Framework Program (FP7/2007-2013) under grant agreement No. 226716.

### **References**

- [1] Ziabicki, A. *J. Chem. Phys.* **2005**, 123, 174103.
- [2] Ziabicki, A.; Misztal-Faraj, B. *to be published*.
- [3] Ostwald, W. *Z. Phys. Chem.* **1897**, 22, 289
- [4] Cheng, S.Z.D.; Zhu, L.; Li, C.Y.; Honigfort, P.S.; Keller, A. *Thermochimica Acta*, **1999**, 332, 105
- [5] Keller, A.; Cheng, S.Z.D. *Polymer*, **1998**, 39, 4461
- [6] Garbarczyk, J. *J.Makromol.Chem.*, **1985**, 186, 145
- [7] Lotz, B. *Polymer*, **1998**, 39, 4561
- [8] Varga, J. *Makromol.Chem., Makromol.Symp.*, **1986**, 5, 213
- [9] Varga, J. *J.Thermal Anal.* **1986**, 31, 165
- [10] Guan-yi, S.; Bin, H.; You-hong, C.; Zhi-qun, H.; Zhe-wen, H. *Makromol.Chem.*, **1986**, 187, 633
- [11] Yoshida, H. *Thermochimica Acta*, **1995**, 267, 239
- [12] Yuan, Q.; Jiang, W.; An, L. *Colloid Polym.Sci.*, **2004**, 282, 1236
- [13] Marigo, A.; Marega, C.; Causin, V.; Ferrari, P. *J. Appl. Polym. Sci.* **2004**, 91, 1008
- [14] Xu, W.; Martin, D.C.; Arruda, E.M. *Polymer*, **2005**, 46, 455

- [15] Garbarczyk, J.; Sterzynski, T.; Paukszta, D. *Polym. Comm.*, **1989**, 30, 153-157
- [16] Garbarczyk, J.; Paukszta, D.; Borysiak, S. *J.Makromol.Sci., part B – Physics*, **2002**, B41, 1267
- [17] Perez, E.; Zucchi, D.; Sacchi, M.C.; Forlini, F.; Bello, A. *Polymer*, **1999**, 40, 675
- [18] "Physical Properties of Polymers Handbook" ed. James E. Mark, American Institute of Physics, Woodbury, New York, **1996**
- [19] Kolodka, E.; Wang, W.; Zhu, S.; Hamielec, A.E. *Macromolecules*, **2002**, 35, 10062
- [20] Billingham, N.C.; Calvert, P.D.; Uzuner, A. *Polymer* **1990**, 31, 258
- [21] Turnbull, D. *J. Appl. Phys.* **1950**, 21, 1022.
- [22] Antonoff, G. *J. Physical & Colloid Chem.* **1948**, 52, 969.
- [23] Gałęski, A. in "Polypropylene: Structure, blends and composites", chapter 4, Ed. J.Karger – Kocsis, Chapman & Hall, London, **1996**
- [24] Monasse, B.; Haudin, J.M. *Colloid Polym.Sci.*, 1985, 263, 822
- [25] Janimak, J.J.; Cheng, S.Z.D. *Polymer Bull.*, 1989, 22, 95
- [26] Li, J.X.; Cheung, W.L.; Jia, D. *Polymer* **1999**, 40, 1219.
- [27] Kolmogoroff, A.N. *Izv. Akad. Nauk SSSR, Ser. Math.*, **1937**, 3, 353
- [28] Avrami, M. *J. Chem. Phys.*, **1939**, 7, 1103; *ibid.* **1940**, 8, 212; **1941**, 9, 17
- [29] Johnson, W.A.; Mehl R.F. *Trans. A. I. M. E.*, **1939**, 135, 416
- [30] Evans, U.R. *Trans. Faraday Soc.* **1945**, 41, 365
- [31] Misztal-Faraj, B.; Sajkiewicz, P.; Savytsky, H.; Bonczyk, O.; Gradys, A.; Ziabicki, A. *Polymer Testing* **2009**, 28, 36
- [32] Magill, J.H. *Nature* **1960**, 187, 770.
- [33] Magill, J.H. *Polymer* **1961**, 2, 221
- [34] Magill, J.H. *Polymer* **1962**, 3, 35
- [35] Ziabicki, A., Misztal-Faraj, B. *Polymer* **2005**, 46, 2395.